Saccharomyces cerevisiae Hop1 Protein Zinc Finger Motif Binds to the Holliday Junction and Distorts the DNA Structure: Implications for Holliday Junction Migration†

Pankaj Tripathi,‡ Debnath Pal,§ and K. Muniyappa*,‡

Department of Biochemistry and Bioinformatics Center, Indian Institute of Science, Bangalore 560012, India

Received June 3, 2007; Revised Manuscript Received August 12, 2007

ABSTRACT: *Saccharomyces cerevisiae* HOP1, which encodes a component of synaptonemal complex, plays an important role in crossing over between homologues. Hop1p contains a zinc finger motif, and substitution of a conserved Cys^{371} by Ser rendered the *hop1* mutant allele defective in sporulation and meiosis. However, the molecular mechanism underlying the function of Hop1 zinc finger motif (ZnF) remains obscure. Here we show that wild-type Hop1 ZnF binds significantly better to the Holliday junction compared with other recombination intermediates. Consequently, the salt titration midpoint for dissociation of the Holliday junction−ZnF complex was higher than the complexes containing flush-ended linear or tailed duplex DNA. Although DNase I footprinting showed that Hop1 ZnF binds to each of the four arms of the junction, $KMnO_4$ probing and 2-aminopurine fluorescence emission data disclosed that it distorts the DNA structure along a pair of symmetrical arms. Molecular modeling studies show that Hop1 ZnF forms a unique zinc-binding fold, reminiscent of the basic helix−loop−helix motif. In the presence of Zn^{2+}, docking studies show that α helix 1, which is replete with basic amino acid residues, makes stabilizing contacts with the sugar−phosphate backbone. Structural comparison revealed a striking similarity between RecG wedge domain and Hop1 ZnF motif. We propose that Hop1 ZnF motif plays a key role in the physical monitoring of recombination intermediates and branch migration of the Holliday junction.

Zinc fingers, one of the most abundant DNA-binding motifs found in eukaryotes, recognize a wide variety of different DNA sequences and regulate a broad range of biological functions (*1*−*4*). Detailed characterization of a relatively small subset of these proteins has implicated ZnF[1] motifs in several cellular functions. Bioinformatics analysis of the human genome estimates approximately 3% of the ∼32 000 predicted open reading frames encode proteins containing zinc fingers (*5*). Similar analysis suggests that 0.7% of the *Saccharomyces cerevisiae* genome potentially encodes zinc cluster proteins (*6*, *7*). Many of these proteins are transcriptional regulators of genes involved in a wide variety of cellular processes including metabolism of compounds such as amino acids and sugars, as well as control of meiosis and multidrug resistance, to name just a few (*8*). In addition, many yeast genes encode putative zinc finger motif-containing proteins whose function is poorly understood. These motifs play a number of different roles, in the catalytic mechanism, or mediate a wide variety of DNA binding, RNA binding, and protein−protein interactions (*1*−*4*). ZnFs are also very important for the structure and function of nucleic acids. The most commonly recognized role of zinc finger motifs is in protein−DNA binding, specifically to G-rich sequences through the major groove, and activation of transcription (*1*−*4*).

A combination of studies has revealed the existence of several families of zinc finger motif-containing proteins (*3*, *4*). Currently, the PROSITE database lists 64 families of zinc fingers such as C_2H_2, C_3H, C_4, and C_6-type zinc finger motifs, based on the number and positions of Cys and His residues. The structure of a typical motif is characterized by folding of a ∼30 amino acid residue peptide into a short two-stranded antiparallel β sheet followed by a α helix with the aid of the Zn^{2+} in a tetrahedral coordination (*1*−*4*). Many natural zinc finger proteins contain multiple DNA binding zinc fingers, but some have as many as 37, joined by small peptide linkers (*1*−*4*). Several lines of evidence indicate that two to three tandem zinc fingers are necessary for specific binding without participation of any other domain. However, there are two exceptions to this general rule: the single zinc finger embedded in the *Drosophila melanogaster* GAGA transcription factor and the QALGGH ZnF motif of the *Arabidopsis thaliana* SUPERMAN protein are capable of sequence-specific DNA binding (*9*, *10*). In both cases, flanking basic

† This research was supported by a grant and by a J. C. Bose National Fellowship from the Department of Science and Technology, New Delhi, to K.M. P.T. is a recipient of Senior Research Fellowship from the Council of Scientific and Industrial Research, New Delhi. D.P. is supported by funds from the Department of Biotechnology, New Delhi, under the Centre of Excellence in Structural Biology and Biocomputing.

* Corresponding author: tel (91-80) 2293 2235/2360 0278; fax (91-80) 2360 0814/0683; e-mail kmbc@biochem.iisc.ernet.in.

‡ Department of Biochemistry.

§ Bioinformatics Center.

[1] Abbreviations: 2-AP, 2 aminopurine; bp, base pairs; BPB, bromophenol blue; BSA, bovine serum albumin; DTT, dithiotreitol; EDTA, ethylenediaminetetraacetic acid; EMSA, electrophoretic mobility shift assays; HJ, Holliday junction; Hop1p, full-length Hop1 protein; Hop1 ZnF, Hop1 protein zinc finger motif; ODN, oligonucleotide, PAGE, polyacrylamide gel electrophoresis; SDS, sodium dodecyl sulfate; SC, synaptonemal complex; ZnF, zinc finger motif.

10.1021/bi701078v CCC: $37.00
Published on Web 10/13/2007

Table 1: Sequences Used in This Study[a]

(A) Sequences of Oligonucleotides Used in This Study	
ODN1	5′ GCCGTGATCACCAATGCAGATTGACGAACCTTTGCCCACGT 3′
ODN2	5′ GACGTGGGCAAAGGTTCGTCAATGGACTGACAGCTGCATGG 3′
ODN3	5′ GCCATGCAGCTGTCAGTCCATTGTCATGCTAGGCCTACTGC 3′
ODN4	5′ GGCAGTAGGCCTAGCATGACAATCTGCATTGGTGATCACGG 3′
ODN5	5′ GCAGTAGGCCTAGCATGACAA 3′
ODN6	5′ TTGACGAACCTTTGCCCACGTC 3′
ODN7	5′ ACGTGGGCAAAGGTTCGTCAATCTGCATTGGTGATCACGGC 3′
(B) Sequences of 2-AP Oligonucleotides Used in This Study[a]	
ODN8	5′ GCCGTGATCACCAATGC**A**GATTGACGAACCTTTGCCCACGT 3′
ODN9	5′ GCCGTGATCACCAATGCAG**A**TTGACGAACCTTTGCCCACGT 3′
ODN10	5′ GCCGTGATCACCAATGCAGATTG**A** CGAACCTTTGCCCACGT 3′
ODN11	5′ GCCGTGATCACCAATGCAGATTGACG**A**ACCTTTGCCCACGT 3′
ODN12	5′ GCCGTGATCACCAATGCAGATTGACGAACCTTTGCCC**A** CGT 3′
ODN13	5′ GACGTGGGCAAAGGTTCGTCAATGG**A** CTGACAGCTGCATGG 3′
ODN14	5′ GCCATGCAGCTGTCAGTCC**A**TTGTCATGCTAGGCCTACTGC 3′
ODN15	5′ GGCAGTAGGCCTAGCATG**A**CAATCTGCATTGGTGATCACGG 3′
ODN16	5′ GGCAGTAGGCCTAGCATGAC**A**ATCTGCATTGGTGATCACGG 3′

[a] Underlined A residues denote positions of 2-AP substitution.

residues providing further contacts with the target sequences stabilize the DNA binding of the finger domain. To our knowledge, ZnF motifs have not been shown to interact with recombination intermediates including the Holliday junction.

S. cerevisiae HOP1, which encodes a component of synaptonemal complex (SC) lateral elements, plays an important role in both gene conversion and crossing over between homologues as well as enforcing checkpoint controls over the progression of meiotic recombination intermediates (*11*−*14*). SC, at least in part, is believed to provide a scaffold for the pairing of meiotic chromosomes along their lengths (*15*). Hop1 protein, which belongs to the family of DNA-binding HORMA (for Hop1p, Rev7p, and MAD2) domain proteins, forms homodimers and hetero-oligomers with Red1 as well as Mek1, and co-inhabits with Red1 discrete sites on axial elements that serve as precursors to lateral elements (*17*−*19*). Genetic and biochemical studies indicate that Hop1 contains a single C_4 zinc finger motif embedded in the center of the 605-residue protein, and substitution of a conserved Cys^{371} by Ser in this motif rendered the *hop1* mutant allele defective in sporulation and meiosis (*11*, *16*, *20*). These findings support the hypothesis that the Hop1 ZnF motif plays a key role in both gene conversion and crossing over between homologues as well as monitoring the progression of meiotic recombination intermediates. Furthermore, characterization of in-frame mutations located at specific sites throughout the *HOP1* open reading frame revealed that Hop1 functions in a multimeric complex (*21*). However, the molecular mechanism by which Hop1 ZnF participates in these nuclear events remains obscure.

Recently, we showed that full-length Hop1 protein binds selectively to the HJ, resulting in DNA conformational changes at the junction (*22*). Bioinformatics analysis of Hop1p sequence disclosed the presence of a putative zinc finger motif (*11*). To gain insights into the role of Hop1 ZnF in full-length Hop1 function, we employed a combination of biochemical, structural, and modeling approaches to examine the function of wild-type and mutant Hop1 ZnF motifs. This approach is especially important for the study of Hop1p because its three-dimensional structure has yet to be determined. In addition, insights into the different modes of interaction of Hop1 ZnF with recombination intermediates will be important for understanding how Hop1p coordinates the processes of crossing over and gene conversion. Biochemical and molecular modeling data indicate that Hop1 ZnF binds to each of the four arms of the junction, while chemical probing and fluorescence emission data disclose that it distorts the DNA structure around the junction along the two symmetrical arms. These results have important biological implications for meiotic recombination since they establish a direct link between Hop1 ZnF and the processes of branch migration and Holliday junction resolution.

MATERIALS AND METHODS

DNA and Hop1 Zinc Finger Motifs. All reagents used were of analytical grade. T4 polynucleotide kinase was obtained from New England Biolabs. Biochemicals and oligonucleotides (Table 1A) were obtained from Sigma. Oligonucleotides (ODNs) were labeled at the 5′ end by use of [γ-^{32}P]-ATP and T4 polynucleotide kinase. Radiolabeled ODNs were purified by electrophoresis on 8% polyacrylamide gels in the presence of 8 M urea. DNA was dissolved in 10 mM Tris-HCl buffer (pH 7.5) containing 1 mM EDTA, and the concentrations are expressed in moles of nucleotide residues. Holliday junctions, Y-shaped substrates, and other intermediates were prepared and characterized as described (*23*, *24*). Briefly, stoichiometric amounts of four purified ODNs were annealed by incubation in 0.3 M sodium citrate buffer (100 μL), pH 7, containing 3 M NaCl for 3 min at 95 °C, followed by slow cooling to 20 °C for 4 h. To prepare HJ, ODN1 was mixed with ODN2, -3, and -4; 3-way junction (ODN2, -3, -5 and -6); 5′-flap (ODN2, -3, and -5); Y-shaped (ODN2 and -3); blunt-end duplex (ODN1 and -7); and 3′-overhang duplex DNA (ODN2 and -6). In the case of 2-AP-containing ODNs (Table 1B), the nonlabeled strands were in slight excess to ensure that the modified strand would be completely incorporated into the HJ. The annealing mixture was electrophoresed on a 6% polyacrylamide gel in 89 mM Tris−borate buffer (pH 8.3) containing 1 mM EDTA at 10 V/cm for 3 h. The annealed bands were excised from the gel, eluted into TE buffer (10 mM Tris-HCl, pH 7.5, and 1 mM EDTA), and precipitated with 0.3 M sodium acetate (pH 5.2) and

95% ethanol. The pellet was washed with 70% ethanol, dried, and resuspended in 20 μL of TE buffer. The identity of recombination intermediates was confirmed by restriction digestion (data not shown). Wild-type and mutant Hop1 ZnF peptides were custom-synthesized by Genemed Synthesis, Inc. The peptides were dissolved in buffer containing 10 mM Tris-HCl (pH 7.5) and 1 mM DTT, and their concentrations were determined at A_{275nm} (ϵ_{275} of Tyr = 1420 M^{-1} cm^{-1} and ϵ_{275} of Cys = 145 M^{-1} cm^{-1}). *S. cerevisiae* Hop1p (*20*) and BLM helicase (*25*) were purified and their concentration was determined as described (*20*, *25*).

Electrophoretic Mobility Shift Assays. Reaction mixtures (20 μL) contained 20 mM Tris-HCl (pH 7.5), 0.1 mM $ZnCl_2$, 5′-^{32}P-labeled DNA (30 nM), 50 mM NaCl, and increasing concentrations of wild-type or mutant ZnF motifs. For homologous and heterologous competition experiments, all components were premixed with the indicated competitor, prior to the addition of Hop1 ZnF, and reactions were incubated for 30 min at 30 °C. Samples were electrophoresed through 8% native polyacrylamide gels in 45 mM Tris−borate (pH 8.3) containing 1 mM EDTA at 10 V/cm for 3−6 h at 4 °C. The gel was dried and exposed to a Fuji PhosphorImager screen, and the bands were visualized by use of the software supplied by the manufacturer. The percentage of bound DNA was determined with UVI BAND MAP and plotted in GraphPad Prism against Hop1 ZnF concentration.

DNA Helicase Assays. Reaction mixtures (20 μL) contained 5′- ^{32}P-labeled HJ (10 nM) 50 mM Tris-HCl (pH 7.5), 50 mM NaCl, 5 mM $MgCl_2$, 5 μg/mL BSA, 2 mM ATP, 1 mM DTT, and indicated amounts of BLM helicase, Hop1p, or Hop1 ZnF. Samples were incubated for 30 min at 30 °C. Reaction was stopped by the addition of stop solution [150 mM EDTA, 2% (w/v) SDS, 30% (v/v) glycerol, and 0.1% (w/v) bromophenol blue]. Samples were loaded onto an 8% polyacrylamide gel and electrophoresed for 3 h at 10 V/cm in Tris−borate buffer (pH 8.3). The bands were visualized as described above.

DNase I Footprinting. DNase I footprinting was performed as described (*28*). Reaction mixtures (20 μL) contained 5′-^{32}P-labeled HJ (100 nM) in 20 mM Tris-HCl (pH 7.5), 0.1 mM $ZnCl_2$, and increasing concentrations of wild-type Hop1 ZnF. Samples were incubated for 30 min at 30 °C. A solution (10 μL) containing 1 mM $MgCl_2$ and 5 mM $CaCl_2$ was added prior to the addition of 0.005 unit/μL DNase I. After 1 min at 24 °C, the reaction was stopped by the addition of 100 μL of stop solution (20 mM EDTA, 5% SDS, 200 mM NaCl, and 25 μg/μL calf thymus DNA). DNA was precipitated with ethanol and resuspended in formamide loading dye [80% (v/v) formamide, 0.1% (v/v) BPB, and 0.1% (v/v) xylene cyanol]. DNA was heat-denatured and analyzed on a 16% polyacrylamide gel containing 7 M urea. The gel was dried and the bands were visualized by autoradiography on Kodak XAR film.

Glutaraldehyde Cross-Linking of Hop1 and Hop1 ZnF. Reaction mixtures (50 μL) contained 20 mM Tris-HCl (pH 7.5), 1 mM $ZnCl_2$, freshly diluted 0.005% glutaraldehyde, and 0.25 μM full-length Hop1 or 5 μM Hop1 ZnF. After incubation at 24 °C for various times, the samples were diluted into gel loading buffer, incubated at 95 °C for 5 min, and analyzed by 7% or 17.5% SDS−PAGE for Hop1p and Hop1 ZnF, respectively. The products were visualized by staining with silver nitrate (*27*).

Fluorescence Measurements. Reaction mixtures contained 20 mM Tris-HCl (pH 7.5), 0.1 mM $ZnCl_2$, HJ (100 nM) bearing 2-aminopurine at indicated positions, and increasing concentrations of Hop1 ZnF in a total volume of 300 μL. Steady-state fluorescence spectra were recorded on a Jobin Yvon (Horiba) Fluromax-3 fluorometer. The emission spectra were obtained by excitation at 315 nm. The emission spectra were recorded in the range of 330−450 nm at 1 nm intervals. The excitation and emission monochromators were set with band passes of 5 and 6 nm, respectively. The emission spectra were corrected for lamp fluctuation and instrumental variation. Tryptophan fluorescence and background emission was corrected by subtractions of control spectra, where 2-aminopurine fluorophore was replaced by adenine. All measurements were performed at 30 °C in a 5 × 5 mm cuvette.

Chemical Probing with Potassium Permanganate. Reaction mixtures (20 μL) contained 20 mM Tris-HCl (pH 7.5), 0.1 mM $ZnCl_2$, 100 nM 5′-^{32}P-labeled HJ, and increasing concentrations of wild-type Hop1 ZnF. Samples were incubated for 30 min at 30 °C. Thymine modification was initiated by the addition of $KMnO_4$ to a final concentration of 1.5 mM, and the samples were further incubated for 2 min at 25 °C. In control reactions, water was substituted for $KMnO_4$. Reaction was quenched by the addition of 50 μL of stop solution [1.5 M sodium acetate (pH 5.2), 1 M 2-mercaptoethanol, and 25 μg/μL calf thymus DNA]. DNA was precipitated with ethanol and collected by centrifugation, and the pellet was dried under vacuum. Modified bases were cleaved with 1 M piperidine (100 μL) for 30 min at 90 °C, and piperidine was removed under vacuum. The A + G molecular weight ladder was prepared as described (*28*). Pellets were resuspended in formamide loading buffer and loaded on a 16% polyacrylamide/7 M urea sequencing gel in Tris−borate buffer. Electrophoresis was performed at 1800 V for 1 h.

Modeling of Hop1 ZnF and Holliday Junction. Two 36-amino-acid peptides, corresponding to the wild-type and mutant sequences of Hop1 protein ZnF motif, were used to model the 3D structure. GENTHREADER (*29*) (http://bioinf.cs.ucl.ac.uk/psipred/psiform.html) was used to assess the putative fold as a helix−loop−helix structure. A similar search with the 3DPSSM algorithm (*30*) also yielded 17 helix−loop−helix patterns among the top 20 results. The *p*-value of the alignments was not significant (>0.5) in both cases, which was not unexpected when the short length of the match is considered. However, a combined assessment of alignments suggests that the results cannot be by chance alone, especially when different sets of proteins are picked up by the two methods. To further check whether indeed any secondary structure other than helix is preferred for the Hop1 ZnF, we used an algorithm that uses only the environment of an amino acid position within a known 3D protein structure to align and score a probe amino acid sequence to a library of templates (*31*). The results showed two top-ranked hits from the Protein Data Bank: 1PB6 and 1TAE spanning helix−loop−helix motifs at a statistically significant *Z*-score of 3.4. We checked other publicly available programs as well, but results of secondary structure prediction and tertiary structure modeling could not accommodate the zinc coordination geometry. Our final structure built on a helix−loop−helix template was corrected for steric clashes and did not have any residue outside the Ramachan-

dran allowed region. There was maximum change in conformation around the loop region for minimizing steric clashes. The model was manually checked for consistency against canonical DNA binding helix−loop−helix motifs (*32*). Presence of positive ϕ torsion in Gly361, burial of hydrophobic residues (Val344, Leu345, Ile375) and (Leu355, Ile358, Leu364, Ile368); and absence of β-branched residue at the wedge position of the helix−loop−helix motif were some of the properties checked.

The PDB template of a three-way DNA junction (1EZM, NMR-derived) was used as a starting block to construct four-way junctions. The duplex at the T base of the three-way junction was truncated, and two such truncated junctions were connected to make a four-way junction. For open-square HJ, the DNA helices were placed approximately in the same plane. For X-stacked-like conformation, the helices were placed such that the approximate angle between the planes containing each of the two DNA helices was 60°. The structures were geometry-optimized to minimize steric clashes. There was minimal cross-helical stacking, with the nearest cross-helical distance between phosphate oxygen at 5 Å near the junction. A three-way junction was preferred as a starting template in place of a four-way junction due to lack of a suitable NMR-derived template or a template derived from DNA junction crystallized without the protein molecule. Such choice of templates was necessary to be consistent with our experimental work involving ZnF and Holliday junction, where the size of the DNA molecule exceeded the protein. The model built was subjected to energy minimization to ensure proper stereochemistry and stable configuration of the molecule. The atoms were assigned Gastieger−Huckel charges for docking studies. The program DOCK (Version 5.2, http://dock.compbio.ucsf.edu) was used scan the docking sites. Briefly, an all-atom representation of the structure was used for the calculations. Default parameters with a flexible ligand and multiple anchors were used for docking. A minimum anchor size of 10 was used to sample as many docking sites as possible. The ligand was not minimized on docking prior to energy calculation. A 6−12 energy potential was used to calculate the van der Waals energy. Chemical scoring was not used. All docked conformations with negative binding energies was short-listed and plotted for evaluation.

RESULTS

Preferential Binding of Hop1 Zinc Finger Motif to the Holliday Junction. S. cerevisiae Hop1 protein zinc finger motif, hereafter referred to as Hop1 ZnF, spans residues $^{348}CX_2CX_{19}CX_2C^{374}$. We generated two 36-mer peptides: the wild-type ZnF motif encompassing residues 343−378 and its corresponding C371S mutant. Previously, we showed that the wild-type peptide, but not the C371S mutant peptide, was able to bind Zn^{2+} at a stoichiometric ratio (*33*). The DNA substrates used in the present experiments encompassed an immobile HJ containing four 20-bp arms; a three-way junction with three 20-bp arms; a flap structure containing 40-bp duplex with a 20-nucleotide 5′-flap single strand; a 40 bp linear duplex DNA; a Y-shaped junction containing a 20-bp duplex region with two 20-nucleotide heterologous single strands; and a 20 bp double-stranded DNA with a 20 nucleotide 3′ single-strand overhang. They were characterized as described (*23*, *34*).

Hop1p binds selectively to the HJ, resulting in DNA conformational changes at the junction (*22*). We have used similar substrates and assays to explore the binding of its putative ZnF to the HJ. The binding of Hop1 ZnF was performed by mixing a fixed amount of radiolabeled DNA with increasing concentration of ZnF and assaying as described under Materials and Methods. Hop1 ZnF was able to form a complex with each DNA substrate. However, Hop1 ZnF bound significantly better to the Holliday junction compared with other recombination intermediates (compare Figure 1, panel A with panels B−G). Control experiments showed that the shifted bands failed to form in the presence of 0.1% SDS and 0.1 mg/mL proteinase K, indicating that slow migration was not due to changes in the secondary structure of DNA (data not shown). Under identical conditions, the C371S mutant peptide failed to bind HJ (Figure 1, panel G) or other types of recombination intermediates (data not shown). The loss of HJ-binding activity of the mutant Hop1 ZnF is consistent with the inability of *hop1* C371S null mutant to complete recombination in vivo (*12*, *13*). Densitometric quantification of DNA−ZnF complexes confirmed the concentration-dependent binding of Hop1 ZnF to the indicated recombination intermediates (Figure 1, panel H). These data indicate that binding of Hop1 ZnF to the HJ and to other recombination intermediates is weak, and the binding preference of Hop-ZnF for HJ > three-way junction ≥ 5′-flap structure > linear duplex ≥ Y-shaped junction ≥ duplex DNA with single-strand overhang. However, peptides have been shown to bind to the HJ with low affinity. Examples of these include hexa- and octapeptides that specifically bind and interfere with the resolution of HJ in λ-integrase and Cre-loxP, Flp-FRT recombination pathways, and resolution of the Holliday junction by vaccinia topoisomerase and *Escherichia coli* RuvABC resolvasome (*35*−*37*).

Under similar conditions, we measured the apparent dissociation constant (K_d) for the formation of the DNA-ZnF complexes as described (*38*). The reaction mixtures contained a fixed amount of the indicated radiolabeled DNA substrate and varying amounts of Hop1 ZnF. Analysis of data showed that K_d values varied significantly with the type of the recombination intermediate. We obtained an apparent dissociation constant of 1.6 μM for the HJ, while it was 2−3-fold higher for other recombination intermediates (Table 2). The sensitivity of peptide−DNA complex to salt is a relative measure of the affinity of the peptide to DNA. The effect of salt on binding was measured by varying the concentration of NaCl in the incubation buffer from 0 to 0.75 M. The data in Figure 2 indicate that the salt titration midpoint for Hop1 ZnF binding to the HJ is ∼0.3 M, whereas it was <0.1 M for the tailed duplex DNA. Competition binding studies confirmed that HJ−ZnF complexes were much more stable in the presence of excess of unlabeled 5′-flap DNA or linear duplex DNA (data not shown). Because of the preferential binding of Hop1 ZnF to HJ, the central intermediate of meiotic recombination, we have chosen to focus on this structure with the wild-type Hop1 ZnF in studies described below.

Hop1 ZnF Impedes the Resolution of Holliday Junction by RecQ Helicase. We have previously demonstrated that binding of Hop1p to the HJ blocked its unwinding by BLM helicase (*22*). We assessed whether binding of Hop1 ZnF

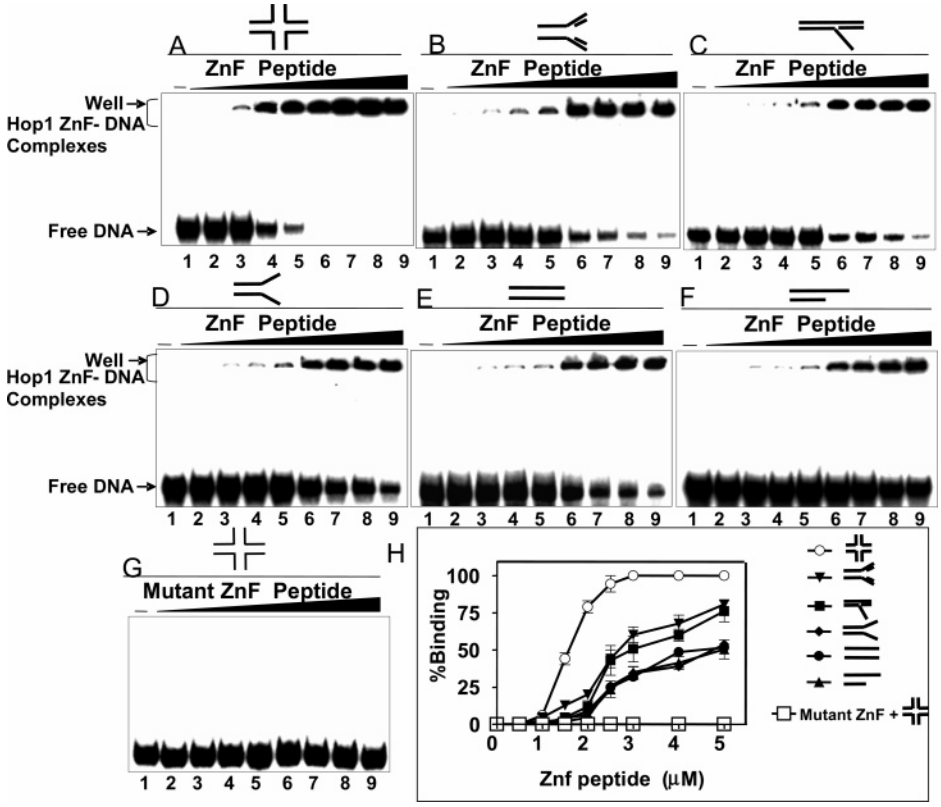

FIGURE 1: Hop1 ZnF binds preferentially to the Holliday junction compared with other recombination intermediates. Reactions mixtures contained 30 nM of the indicated 5′-^{32}P-labeled substrate in the absence (lane 1) or presence of 0.5, 1, 1.5, 2, 2.5, 3, 4, or 5 μM wild-type or mutant Hop1 ZnF motif (lanes 2−9, respectively). The symbol on top of the gel image denotes increasing amounts of wild-type or mutant Hop1 ZnF motifs. Reaction products were separated as described under Materials and Methods. **(**A) HJ; (B) 3-way junction; (C) 5′-flap; (D) linear duplex DNA; (E) Y-shaped DNA; (F) 3′-tailed duplex DNA; (G) HJ in the presence of hop1 mutant ZnF motif. The positions of free DNA and Hop1 ZnF−DNA complexes are indicated on the left-hand side. (H) Graphical representation of Hop1 ZnF binding to different recombination intermediates. The extent of formation of Hop1 ZnF−DNA complex in panels A−G is plotted against varying concentrations of Hop1 ZnF. Error bars indicates SEM.

Table 2: Dissociation Constants for Hop1 ZnF Motif Binding to Different Recombination Intermediates

DNA structures	K_d (μM)
Four way junction	1.56 ± 0.15
Three way junction	2.73 ± 0.28
5' -Flap	2.84 ± 0.21
Y-Shaped Junction	4.79 ± 0.35
Duplex	4.83 ± 0.38
3'-Overhang	4.95 ± 0.31

inhibits unwinding of HJ by BLM helicase by using an assay that measures the resolution of HJ into various intermediates. We incubated HJ, radiolabeled at the 5′ end of all four strands, with increasing concentrations of BLM helicase. The reaction products were resolved by PAGE and visualized by autoradiography. Control reactions showed that 10 nM BLM helicase was able to convert nearly all of the HJ into unwinding intermediates (Figure 3, lane 4). In such an assay, Hop1p blocked unwinding of the HJ in a concentration-dependent manner (Figure 3, lanes 5−8). Similarly, Hop1 ZnF was able to confer protection to HJ against unwinding but required substantially higher concentrations (Figure 3, lanes 9−12). Importantly, Hop1p and its ZnF produced an identical pattern of intermediates. For comparison, we also tested the ability of Hop1 ZnF mutant to confer protection to HJ and observed that it was unable to inhibit unwinding by BLM helicase (data not shown). These results corroborate with the gel mobility data and confirm specific interaction of Hop1 ZnF with HJ.

Correlation of Weak Binding to the Oligomerization State of Hop1 ZnF. Having demonstrated the ability of Hop1 ZnF to interact with HJ, we next explored the possible structural basis for the low specificity of Hop1 ZnF to the HJ and other recombination intermediates (Table 2). One possibility is that protein−protein interactions outside the Hop1 ZnF might contribute to robust binding and substrate selectivity. The low selectivity therefore might result from the absence of other domains of the Hop1p. Genetic studies have shown that interactions between Hop1 monomers are important for its function (*21*). Consistent with the in vivo correlates, our in vitro findings showed that Hop1 dimer is the stable form in solution and oligomerization increases its affinity to DNA (*20*). Therefore, it remained possible that weak binding of Hop1 ZnF to the HJ may directly result from its inability to form stable homodimers or oligomers. The potential for homodimerization of Hop1p and Hop1 ZnF was addressed by covalent protein−protein cross-linking with glutaraldehyde. Figure 4 shows that, in the presence of glutaraldehyde, Hop1p was able to form homodimers. However, under similar conditions, Hop1 ZnF remained monomeric even after

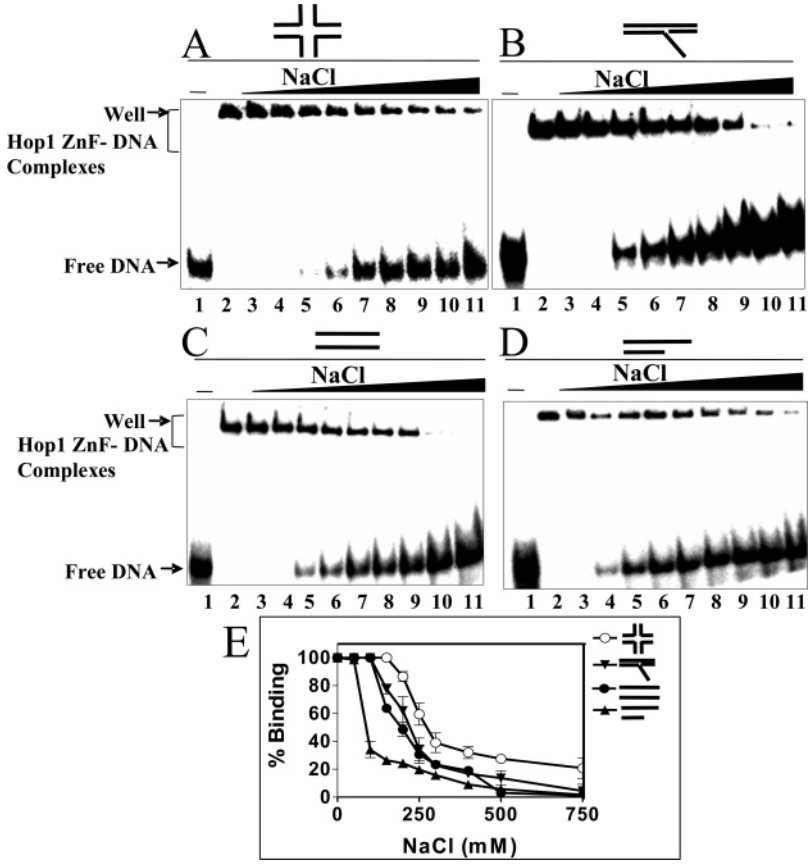

FIGURE 2: Effect of NaCl on the stability of Hop1 ZnF−DNA complexes. Reaction mixtures contained 30 nM of the indicated 5′-^{32}P-labeled DNA substrate and 1 μM Hop1 ZnF motif. After incubation for 30 min, additional NaCl was added to a final concentration of 0.05, 0,1, 0.15, 0.2, 0.25, 0.3, 0.4, 0.5, or 0.75 M (lanes 3−11, respectively). After 10 min with NaCl, samples were electrophoresed on a polyacrylamide gel and visualized by autoradiography as described under Materials and Methods. (E) Extent of dissociation of Hop1 ZnF−DNA complex containing the indicated recombination intermediate is plotted against varying concentrations of NaCl. Error bars indicate SEM.

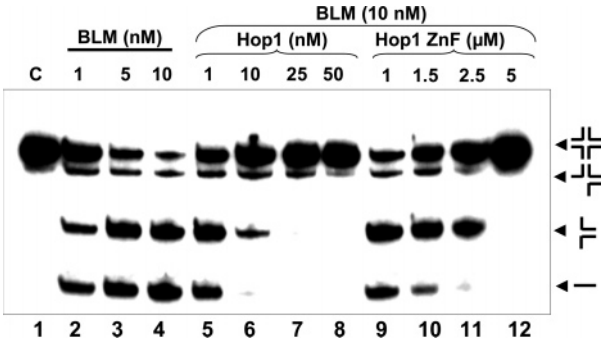

FIGURE 3: Hop1p or Hop1 ZnF impedes the resolution of Holliday junctions by BLM helicase. Reaction mixtures contained 10 nM 5′-^{32}P-labeled HJ (lane 1) and the specified concentrations of Hop1p or Hop1 ZnF and BLM helicase as indicated at the top of each lane. The products were separated by PAGE as described under Materials and Methods. The structures of different intermediates generated in the course of the dissolution of HJ are shown on the right-hand side.

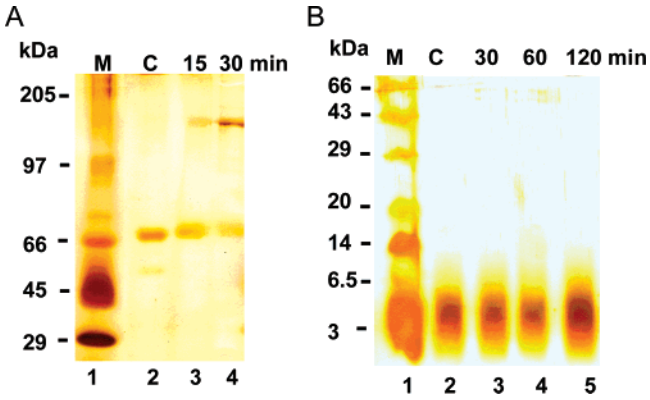

FIGURE 4: Glutaraldehyde cross-linking. (A) Cross-linking of Hop1p. The reactions were performed as described under Materials and Methods. Lane 1, molecular weight standards; lane 2, Hop1p incubated for 30 min in the absence of glutaraldehyde; lanes 3 and 4, full-length Hop1 incubated with 0.005% glutaraldehyde for the indicated time intervals. (B) Cross-linking of Hop1 ZnF motif. Lane 1, molecular weight standards; lane 2, Hop1 ZnF incubated for 2 h in the absence of glutaraldehyde; lanes 3−5, Hop1 ZnF incubated with 0.005% glutaraldehyde for the indicated time intervals. The positions of different molecular weight standards are shown on the left-hand side.

2 h of incubation. Taken together, we propose that Hop1 binding to DNA involves a bipartite substrate recognition mechanism: the ZnF is the principal structural determinant involved in DNA binding, while other domains of Hop1p may serve to provide DNA structure selectivity and stability.

Hop1 ZnF Binds to the Core of a Holliday Junction. The Holliday junction free in solution is structurally polymorphic (*36*−*38*). In low-salt buffers and in the absence of divalent cations, HJ extends into open conformation. On the other hand, the Holliday junction folds into a stacked X-structure in the presence of divalent cations. In the latter, two of the strands run continuously through a given pair of stacked helices, whereas the other two stands are exchanged between helical pairs (*39*−*41*). We performed DNase I footprinting

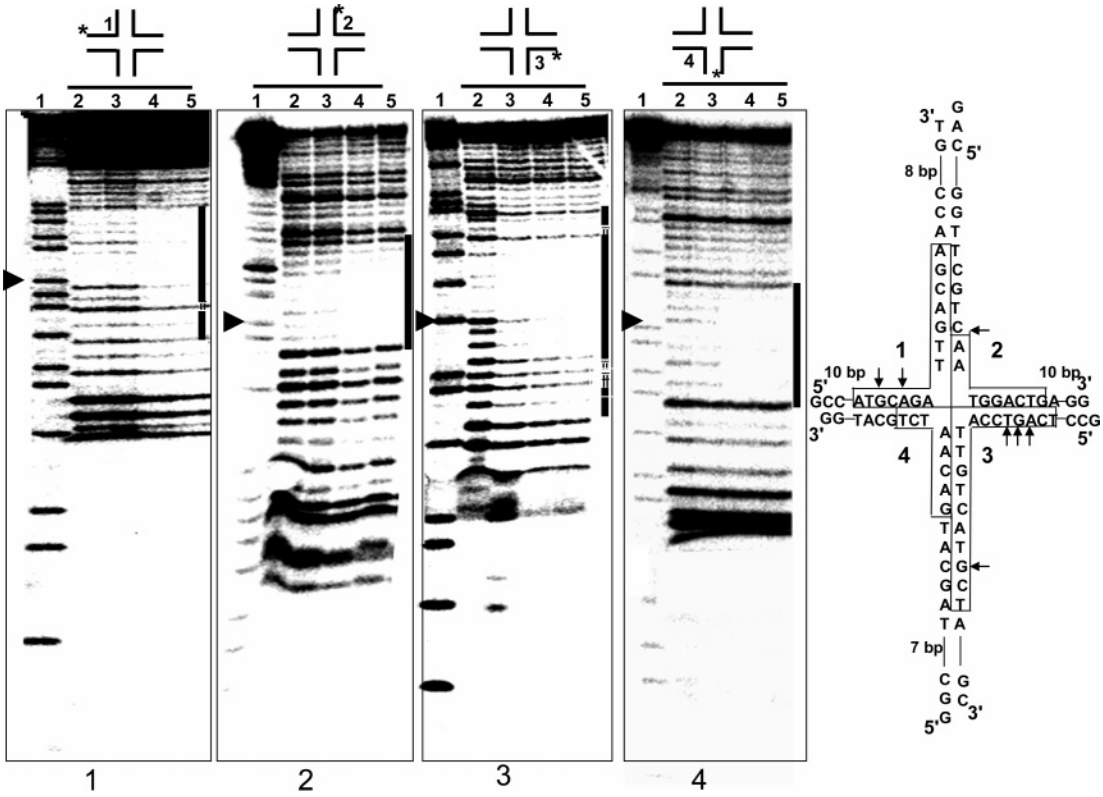

FIGURE 5: DNase I footprinting of Hop1 ZnF motif−HJ complexes. Reaction mixtures contained 100 nM HJ, radiolabeled on the strand as indicated by asterisks, in the absence (lane 2) or in the presence of 1, 2.5, or 5 μM Hop1 ZnF motif (lanes 3−5). The reaction was initiated by addition of DNase I, and the products were separated as described under Materials and Methods. Lane 1, Maxam−Gilbert sequencing reaction (G + A). The arrowhead on the left-hand side of each panel denotes the HJ crossover point. The region of protection from DNase I digestion is indicated by vertical solid bars on the right-hand side of each panel. The HJ diagram on the right-hand side depicts regions of protection (in the box). Arrows denote the residues that are not protected from DNase I cleavage.

to examine the site of binding of Hop1 ZnF to the Holliday junction. Each strand of HJ DNA radiolabeled at the 5′-end was analyzed independently in the absence or presence of increasing amounts of Hop1 ZnF. The reaction conditions were essentially the same as for the EMSA except that the binding buffer contained 1 mM $MgCl_2$. All four strands of HJ DNA showed regions of protection, and the extent of protection increased with increasing amounts of Hop1 ZnF. Although the extent and pattern of protection showed strand variability, a clear region of protection was evident on both 5′ and 3′ sides of the HJ center (Figure 5, lanes 3 and 4). However, the area of protection is more extensive on the exchanging strands (Figure 5, strands 1 and 3) than the continuous strands (strands 2 and 4). The overall size of the Hop1 ZnF footprint is in the range of 9−18 bp. Examination of the protected regions revealed approximately 4-fold symmetry around the junction center.

Chemical Probing of Hop1 ZnF−Holliday Junction Complex. To determine whether chemical probing can distinguish between the small and the extended protection patterns observed with DNase I, we examined the sensitivity of HJ to $KMnO_4$ upon binding of Hop1 ZnF. Since the base-paired T residues are insensitive to oxidation by $KMnO_4$, this approach is likely to provide insights into helical distortion of the HJ (*42*). Each strand of HJ DNA radiolabeled at the 5′-end was incubated with ZnF and then probed with $KMnO_4$. In control experiments, the T residues were insensitive to reaction with $KMnO_4$ (Figure 6). On the other hand, central T bases in Hop1 ZnF−HJ complexes showed selective reactivity, and the efficiency of the reaction increased with increasing Hop1 ZnF concentrations (Figure 6, panels 1−4, lanes 6−9). Strikingly, the pattern of $KMnO_4$ modification revealed two important features. First, the reactive T residues are located principally around the center of the junction; and second, sensitivity of T residues extended >4 bp from the junction center in the two symmetrical duplex DNA arms, thus culminating in approximately 2-fold symmetry.

Hop1 ZnF Distorts the Structure of a Holliday Junction. To gain further insights into the mechanism underlying the action of Hop1 ZnF, we used 2-aminopurine (2-AP) as a fluorescent reporter of changes in base-pairing interactions. The fluorescence of 2-AP when substituted for the normal base is often an effective probe to measure helical distortions, as the fluorescence is heavily quenched in a DNA duplex. This has been extensively used to examine helix opening by HJ-binding proteins (*43*, *44*). We used nine HJ substrates, each containing a single 2-AP substitution at the sites highlighted within open squares (Figure 7, central structure in upper panel). The fluorescence emission spectra of HJ bearing 2-AP at a site immediately 3′ to the center were recorded as a function of increasing amounts of Hop1 ZnF. The spectra showed an increase in 2-AP fluorescence by ~4-fold and then plateaued (Figure 7, small panel A). Similar analyses were carried out with each HJ containing 2-AP at different sites. We found a significant increase in fluorescence emission with HJs containing 2-AP 5′ to the junction center.

Figure 7 (lower panel) shows the fluorescence intensity as arbitrary units against increasing concentration of Hop1 ZnF or its mutant variant at 367 nm. We found an increase

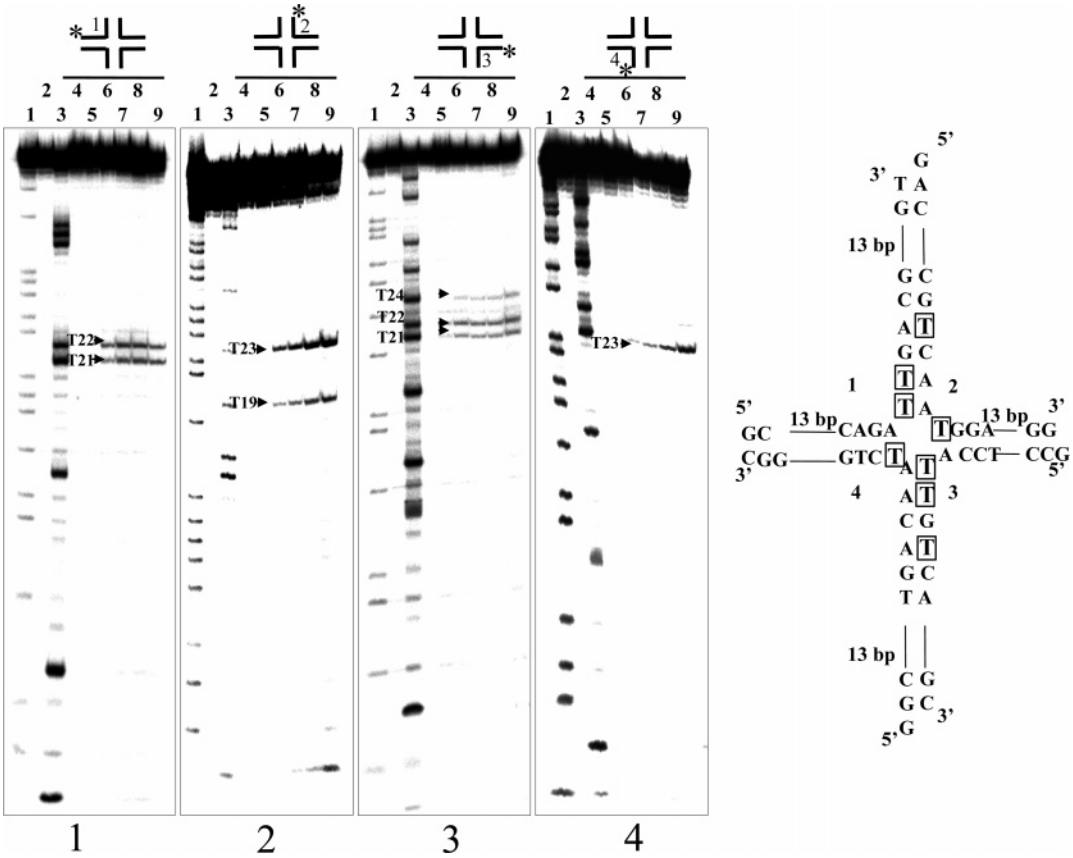

FIGURE 6: Sensitivity of Hop1 ZnF motif−HJ complex to oxidation by $KMnO_4$. Reactions were performed with 100 nM linear duplex or HJ, radiolabeled in strand 1, strand 2, strand 3, or strand 4 in the absence (lane 4) or presence of Hop1 ZnF motif (lanes 6−9), respectively. Samples were treated with $KMnO_4$ and the products were resolved on a 15% polyacrylamide−urea denaturing gel. Lane 1, A + G ladder; lane 2, HJ substrate; lane 3, T ladder; lane 4, treated with $KMnO_4$ in the absence of Hop1 ZnF; lane 5, HJ incubated with 2.5 μM Hop1 ZnF motif but not treated with $KMnO_4$; lanes 6−9, complete reaction containing Hop1 ZnF at 0.50, 1, 2.5, and 5 μM, respectively. The HJ diagram on the right-hand side depicts T residues (square box) rendered sensitive by Hop1 ZnF motif.

in fluorescence emission, up to 4-fold, with HJs containing 2-AP immediately 5′ to the junction center. Likewise, an increase in fluorescence emission was also evident with HJ substrates containing 2-AP, up to 4 bp, inside the two symmetrical arms. On the other hand, fluorescence was measurable but less pronounced with HJs containing 2-AP 3 bp inside a pair of symmetrical arms (Figure 7, lower panel). These results, consistent with chemical probing, suggest that although Hop1 ZnF binds to the junction with a 4-fold symmetry (Figure 6), it distorts the DNA structure in a 2-fold symmetric fashion.

Hop1 ZnF Has a Unique Helix−Loop−Helix Zinc Finger Fold. In order to complement our experimental work on the interaction of Hop1 ZnF with the HJ, we carried out molecular modeling studies. A number of secondary structure prediction methods were used to assess tertiary structure of the Hop1 ZnF consistent with zinc-binding topology. Among these studies, only the structure derived from GENTHREADER (*25*) and 3D PSSM (*30*) showed a majority of helix−loop−helix motif structures (Figure 8). The statistically significant *Z*-score of the match, using fold recognition algorithm of Mallick and colleagues (*31*), is significant when the short length of the match is considered. Closer examination of the tertiary model (Figure 9A) revealed the unique hallmarks of a DNA binding helix−loop−helix motif (*32*). Interestingly, like Hop1 ZnF, the zinc fingers in ribosomal proteins L37 and L37a (*45*) and in GATA-1 transcriptional activator, which contain Cys_4 zinc fingers, do not fold into helix−loop−helix structures. In fact, most of the zinc fingers known to date fall into the $\beta\beta\alpha$ fold, although helix−loop−helix structures are ubiquitous DNA-binding elements in all kingdoms of nature. For most of the known helix−loop−helix domains, the helices are found almost at 90° to each other (*46*). The zinc coordination in conjunction with the predicted (GENTHREADER) helix−loop−helix structure precludes such a possibility, and helices 1 and 2 run almost parallel to each other (Figure 9A). Such parallel-aligned helix−loop−helix motifs are found, though less frequently, and none of them are stabilized by zinc coordination. The closest structure this zinc finger resembles in topology is the Taz2 domain (*47*), where the zinc coordination is C_4 in DNA polymerase II subunit γ (PDB code 1JR3; ref *48*), but here the protein segment anchored between the zinc-coordinated cystines is too short (eight residues) to form any secondary structure element other than a loop. Therefore, Hop1 protein bears a unique zinc finger motif reminiscent of the basic helix−loop−helix motif.

Modeling Studies Suggest Interaction of Hop1 ZnF at the Junction Center. Docking scans on HJ models show that the frequency of docking with stable (negative) binding energy is higher around the junction, compared to the arms where the DNA exists as pure duplex. Figure 9B shows that although the junction region only covers about $^1/_3$ of the total number of nucleotides in the molecule, the number of docking sites detected is about 50% of the total sites found in the whole molecule. This suggests that the intrinsic binding

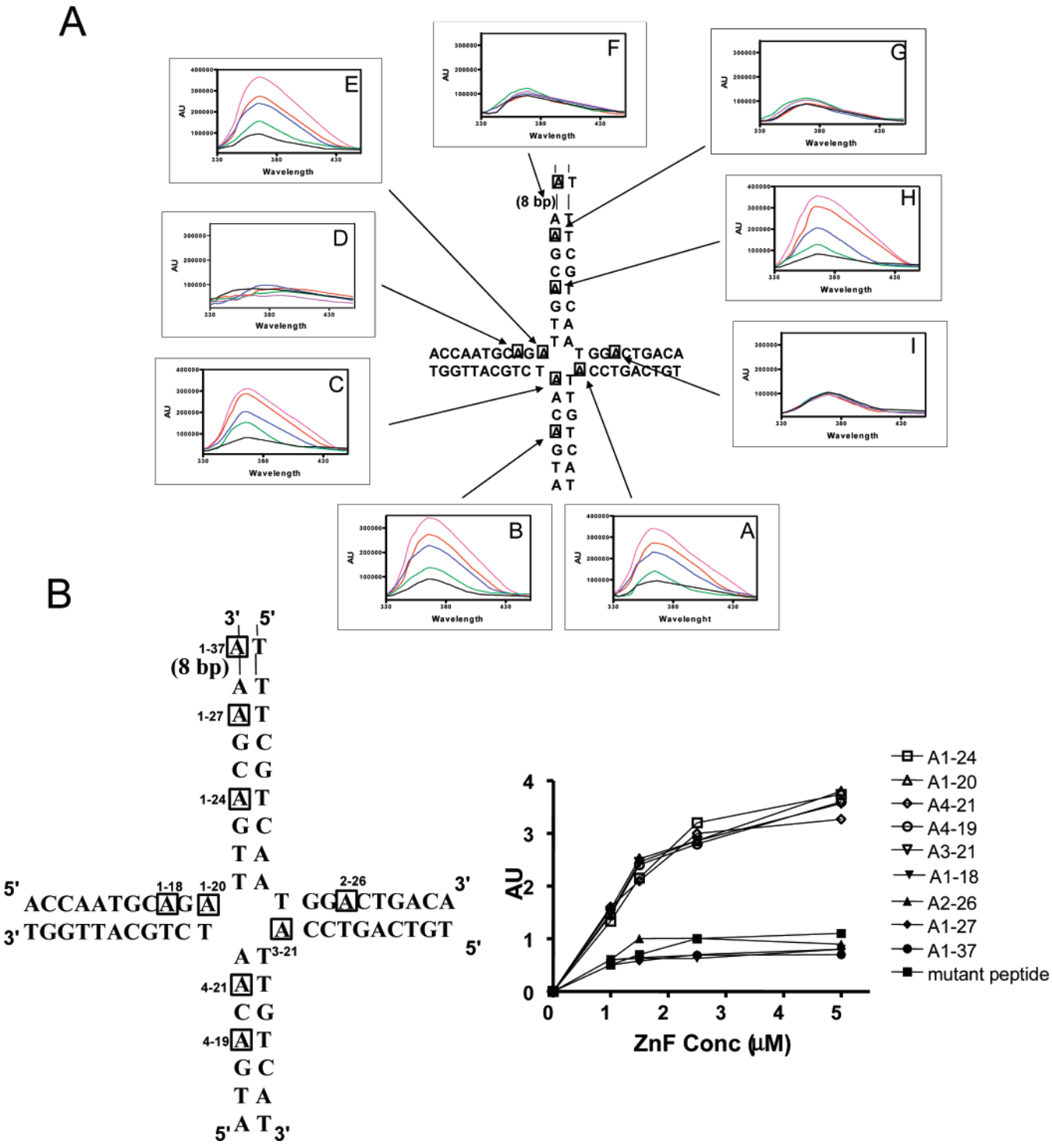

FIGURE 7: Hop1 ZnF motif induces structural distortion of the Holliday junction. (Upper panel) Relevant region of the HJ with its base sequence is depicted in the center. The positions of the adenine bases, which were individually substituted with 2-AP, in all four strands are shown within boxes. The corrected fluorescence emission spectra were recorded in the wavelength region between 330 and 450 nm. The *y*-axis (in arbitrary units) represents fluorescence intensity changes of 100 nM HJ in the absence (black) or presence of 1 μM (green), 1.5 μM (blue), 2.5 μM (red), and 5 μM (purple) of Hop1 ZnF, respectively, in the wavelength range 340−390 nm (*x*-axis). Fluorescence emission spectrum of each HJ variant has a black arrow pointing to the corresponding 2-AP residue in the HJ diagram depicted at the center. Differences in the emission intensities are apparent in the range between 340 and 390 nm. (Lower panel) Relevant region of the HJ with its base sequence is depicted on left-hand side. The positions of the adenine bases, which were individually substituted with 2-AP, in all four strands are shown within the square boxes. The *y*-axis represents fluorescence intensity changes (in arbitrary units);the *x*-axis represents the concentration of Hop1 ZnF.

potential of the zinc finger around the junction is much higher. This may be attributed to more potentially stabilizing contacts around the junction, compared to elsewhere. This could be the reason why the average binding energies for docking around the junction are more negative (stable) than elsewhere. It is instructive to note that all DNA-binding helix−loop−helix motifs are known to interact with the major groove, and the contacts are on the exposed surface

```
Hop1_Zinc1  :343 TVLKTCKSCRKTLHGICYGNFLHSSIEKCFTCIPGP 378
1xouB(25.0%):046 TDPQAAEKLNKLIEGYTYGDSALSKIEKLIETL--- 084
1jplA(27.8%):071 TVLEACKNCGRRFHNEV-GKF--RFLNELIKVV-SP 104
1v4gA(19.4%):408 DLFRDLKRVAQTLDSINGGEAYQKVCDELVACFDNP 443
1sis0(31.4%):011 NMAKKCRDC-------CGGN------GKCF----GP 029
1erd0(33.3%):004 TCEQAMASCEHTMCGYCQGPLY-------MTCICGP 040
1j0tA(25.0%):020 KVVRVCEDCTNILDGMCRNR--------CFICLKAA 058
1hp80(16.7%):012 CEIQKCSKCQAVI----------QELRKC--CAQYP 043
2occH(13.9%):018 NQTRNCHRCEKAMVSVC------EWYRRVYKSLC-P 059
1fn9A(22.2%):288 KGTAKLKTVRKLVEAVNWG------VEK-IRYALGP 318
1gw5A(5.6%) :374 RDVSVRQRAVDLLYAMCDRSNAQQIVAEMLSYLETA 409

Hop1_Zinc1  :343 TVLKTCKSCRKTLHGICYGNFLHSSIEKCFTCIPGP 378
1mmh6(25.0%):233 ------KSLAIIVGALC---WLPLHIINCFTFFC-P 260
1erp0(16.7%):001 ---DLCEQCEQGCHNFCSP----EDKPGCLGMVLCP 038
1hwtC(19.4%):059 RIPLSCTICRKRKVK-CDKL--RPHCQQCTKCHYME 097
1erd0(27.8%):001 -DPMTCASCEHTMCGYCQGPLYMTCIGITTDPECGP 040
1cld0(19.4%):093 ---QACDACRK--KKWCSKT-----VPTCTNCLYS- 125
1fmhB(08.3%):001 ----EVQALKKRVQALKARNYAAKQKVQALRHKCG- 031
1ddd5(16.7%):204 ----FVYSMCTTVFMFC---IPFIVILGCYGLIVKA 232
1gngY(08.3%):198 -------DPHRLLQQLVLGNLIKEAVRRLHS----- 222
1mmh4(16.7%):116 ----TGTRAKGII-AIC----WVLSFAIGLTPMLGW 143
1tiiC(25.0%):195 ---TTCASLTNKLSQHDLADF-KKYIKRKFTSINN- 230
1cosA(13.9%):001 ----EWEALEKKLAAL---ESKLQALEKKLEALHG- 029
1d66A(22.2%):008 --EQACDICRLKKLK-CSKE--KPKCAKCLECRYSP 048
1eciA(16.7%):001 GVIKIWETVCPTVEPWCSGDIATYIKRECGKL---- 037
1eciB(19.4%):001 --WSTLTICLKSMAKKCEGSIATMIKKKCDK----- 034
1qp6A(13.9%):001 ---GEVEELEKKFKELWKGGEIEELHKKFHELIKG- 035
2pf10(13.9%):036 ----SATDAFWAKYTACES--ARNPREKLNECLEGN 065
```

FIGURE 8: (Upper panel) Analysis from the GENTHREADER[28] server, shown as consensus multiple alignments. On the left the PDB code is given by a 4-letter code followed by the chain identifier. If no chain identifier exists, it is represented as 0. The percentage match of the template is given in parentheses, as are the start and the end positions in the alignment. In the top panel the Cys residues that bind zinc are marked by asterisks. The residues predicted to be in helical conformation in ZnF and observed as helical residues in templates are represented in boldface type. If two residues from the template are noncontiguous in the alignment, they are underlined. A hyphen denotes a gap, and regular letters indicate residues with nonregular secondary structure. (Lower panel) Same results from 3DPSSM (*26*).

and around the tip of the helix and residues in the neighborhood. In our docking results the contacts made by the helices are consistent with this experimental observation; however, the DNA binding sites are not always in the major grooves. Examination of individual docked Hop1 ZnF motifs in the junction region suggests complementary interaction with the major groove that ingresses into the DNA junction. Hop1 helix 1, which is replete with basic amino acids, makes most of the stabilizing contacts with the sugar−phosphate backbone in a nonspecific manner. The location of Hop1 ZnF binding to the HJ has an inherent structural symmetry evident from the $KMnO_4$ probing (Figure 6) and 2-AP fluorescence emission measurements (Figure 7). The binding contacts appear to favor only two of the four arms of the HJ. This can be explained from the geometry of the strands in the HJ. The strands that are exchanged across helices show larger contact and opening upon association with Hop1 ZnF compared to the strands that remain same in the same helix. As shown in Figure 9B, strands 2 and 4 do not branch-migrate across helices and therefore show minimal interaction with the Hop1 ZnF motif.

Hop1 ZnF Motif Shows a Striking Similarity to RecG Wedge Domain. In many eubacteria, the RuvAB and RuvC proteins have been shown to catalyze branch migration and resolution of the Holliday junction (*44*). In addition to the RuvABC resolvasome, eubacteria possess a very highly conserved helicase, RecG, which specifically binds HJ and replication forks and catalyzes branch migration (*44*). RecG is absent from all eukaryotes except for some plants (*44*). The crystal structure of *Thermatoga maritima* RecG in complex with a three-way DNA junction reveals three structural domains: a large N-terminal domain and two helicase domains (*49*). The center of the N-terminal domain adopts an OB-fold, referred to as the wedge domain, which makes extensive contacts to both strands of the single-stranded DNA at the template junction. Analysis of the crystal structure identified two amino acid residues in the wedge domain that are critical for DNA binding: Phe^{204} and Tyr^{208} (*49*, *50*). The isolated *E. coli* wedge domain bound Holliday junction with high affinity, indicating that the wedge domain establishes strong binding at the HJ branch point (*50*, *51*). Interestingly, comparison between Hop1 ZnF and RecG wedge domain show that the arrangement of aromatic amino acid residues Tyr^{360} and Phe^{363} in the loop region of Hop1 ZNF is similar to that of Phe^{204} and Tyr^{208} in the RecG wedge domain loop (Figure 10). The aromatic rings are suitably juxtaposed to recognize individual bases in the junction regions of the recombination intermediates. These results are consistent with the ability of Hop1 ZnF to establish strong binding at the HJ core and distort its structure. The possibility of whether Hop1, or its ZnF motif, functions as a helicase analogous to RecG is currently under investigation.

DISCUSSION

In this study, we show that Hop1 ZnF binds preferentially to the Holliday junction compared with other types of recombination intermediates. Consistent with the genetic studies, substitution of a conserved Cys with Ser in the Hop1 ZnF completely abolished its binding activity to all the recombination intermediates. DNase I footprinting data revealed that Hop1 ZnF binds to the central core of the Holliday junction with nearly 4-fold symmetry. Molecular modeling also demonstrated that Hop1 ZnF associates at the core of the HJ junction. It is logical, therefore, to assume that, upon binding to HJ with 4-fold symmetry, Hop1 ZnF might distort the structure equally in all four arms. Remarkably, chemical probing and 2-AP fluorescence emission measurements indicate that structural distortion culminates in nearly 2-fold symmetry. On the basis of these findings, we propose that repeated distortion of the junction center might drive unidirectional branch migration and generation of heteroduplex DNA.

Recently, we showed that native Hop1 protein binds selectively to the HJ, resulting in pronounced structural distortion of the junction (*22*). Comparison between the activities of Hop1 ZnF and Hop1p revealed several important features intrinsic to the ZnF motif. First, the minimal region of Hop1p required for binding to the HJ is the ZnF motif. To our knowledge, this is the first example of specific binding and structural distortion of HJ by a ZnF motif, thus revealing a new function for zinc finger motifs. Second, Hop1 ZnF displays the ability to discriminate among closely related substrates, consistent with its role in the progression of meiotic recombination intermediates in vivo (*12*). Third, whereas Hop1p was able to form homodimers, Hop1 ZnF remained monomeric; this has implications for DNA structure selectivity. Fourth, molecular modeling studies showed that Hop1 ZnF motif forms a novel zinc-binding fold, reminiscent of the basic helix−loop−helix motif. Finally, structural comparison revealed a striking similarity between RecG wedge domain and Hop1 ZnF motif. All of these observations support the notion that Hop1 ZnF motif is sufficient to

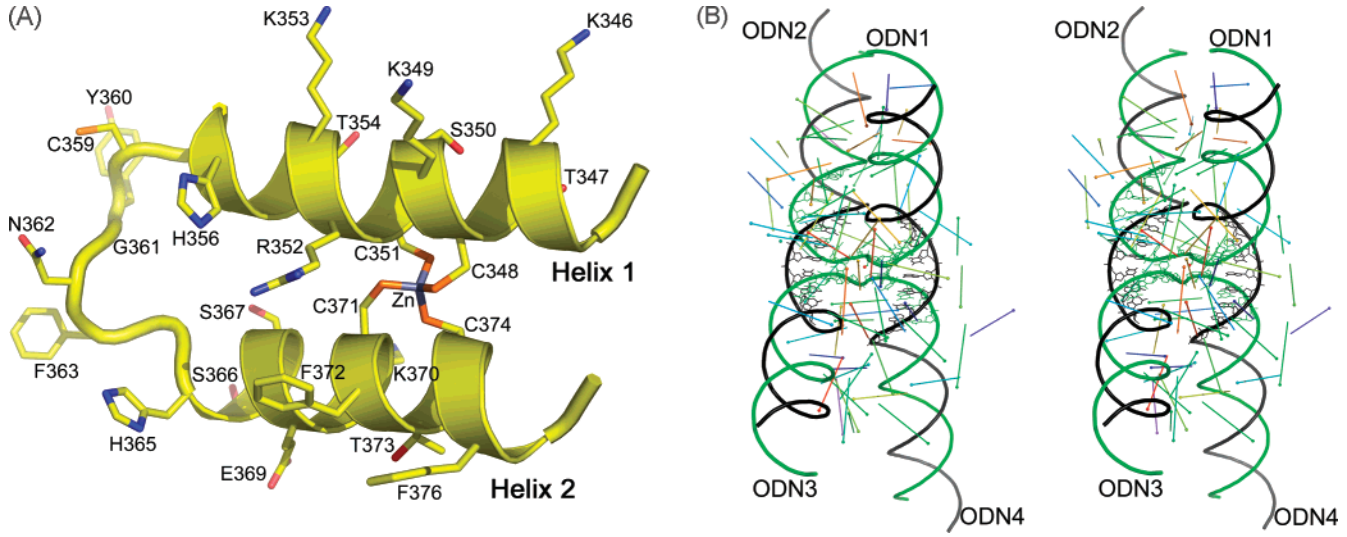

FIGURE 9: (A) Putative three-dimensional model of the Hop1 ZnF motif based on alignment shown in Figure 8. The two helices are separated by a loop. The first helix (Helix 1) is distinctly basic with three Lys, one Arg, and one His residue. Residues deemed important for interaction are labeled (one letter amino acid code and the position in the sequence). The distance of the zinc atom to the Cα atom position in Gly^{361} is approximately 17 Å. **(B)** Putative three-dimensional model of HJ showing X-stacked-like conformation with the two B-DNA helices aligned at around 60°. Strands 2 and 4 (marked ODN2 and -4, shown in black) wind unidirectionally to form a B-helix, while strands 1 and 3 (shown in green) form a junction and exchange across helices. The molecule is approximately 40 Å in width around the junction. The part of the junction found to interact with the zinc finger is highlighted in ball-and-stick format. The rounded arrows indicate the zinc finger and their docking orientation obtained from the DOCK program. The tail of the stick starts at the position of the Zn^{2+} atom and the head, marked by a sphere, represents the Cα atom of the Gly^{361} residue. The color of the stick varies from red to green to blue corresponding to a linear gradient of binding energy from −134.9 to −17.6 kcal/mol. The frequency of docked Hop1 ZnF motif is higher around the junction than elsewhere.

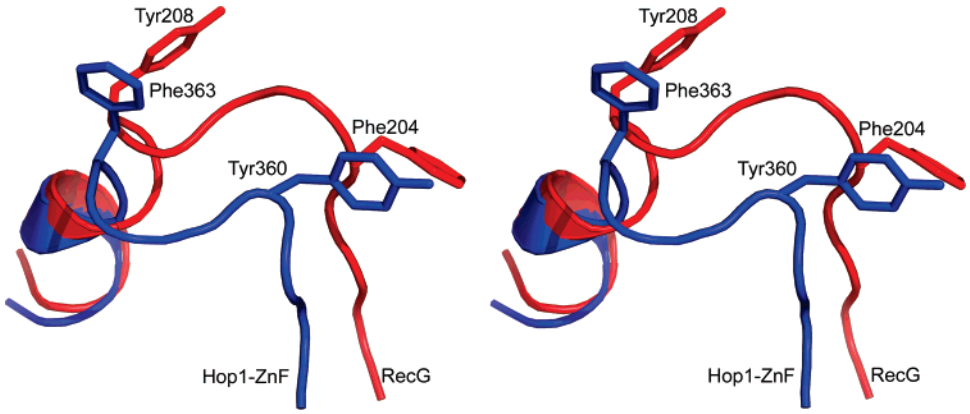

FIGURE 10: Structural comparison of the Hop1 ZnF motif (blue) with the loop region of RecG wedge domain (red). The Hop1-ZnF residues from 357 to 369 and the wedge domain residues 200−215 (PDB code 1GM5, chain A) were superposed by use of four helical residues at the C-termini of the respective polypeptide chains. The figure was drawn with the program PyMOL (*60*).

interact with the HJ and impose conformational changes on its structure.

The present studies were carried out to explore the ability of Hop1 ZnF to bind and discriminate among a set of meiotic recombination intermediates. Specifically, we asked whether Hop1 ZnF directly interacts with HJ and functionally mimics the full-length native Hop1 protein. The data presented here indicate that Hop1 ZnF specifically binds to the junction center, but the affinity constant is rather high. This result contrasts with the dissociation constants determined for the interaction of peptides containing a minimum of two widely separated zinc finger motifs with their target DNA sequences (*52*−*54*). However, the K_d values determined here for the interaction of Hop1 ZnF with HJ is comparable to those reported for the binding of peptides to the HJ (*35*−*37*). In contrast to the Hop1 ZnF, however, $KMnO_4$ probing showed that hexapeptides do not cause distortion of DNA helix inside the HJ arms (*37*). Although affinity, as reflected through K_d values, is ideally determined for the native full-length protein, such measurements for short synthetic peptides tend not to be closer to the actual values. For example, a peptide corresponding to GAGA factor, containing a single zinc finger motif but lacking the flanking stretches of basic amino acid residues, failed to bind DNA (*9*, *55*, *56*). Similarly, the *A. thaliana* SUP single zinc finger motif is stabilized by flanking basic amino acid residues (*10*).

Analyzing the molecular modeling data drives us to an important interpretation of the topology of Hop1 ZnF. In contrast to numerous zinc finger family members, the Hop1 ZnF folds into a unique zinc finger motif. We assume that the isolated Hop1 ZnF itself retains the same fold as that in the native protein. The structures of isolated single or double ZnF motifs in solution are remarkably similar to the crystal structures of native proteins (*57*, *58*). A survey of the

structural features of zinc finger motifs in the literature has revealed the existence of eight groups, defined on the basis of structural properties in the vicinity of the zinc-binding site (*47*). All zinc fingers that belong to the same fold group have zinc ligands in a similar structural context. Structural studies carried out with classical zinc finger−DNA complexes have revealed that sequence-specific recognition is achieved by contacts between the amino acid residues in the α helix of the zinc finger and bases in the major groove of the DNA. However, a structural feature that distinguishes Hop1 ZnF from its counterparts is that the four cysteines from two α-helices tetrahedrally coordinate a zinc ion to form a compact structure. In addition, molecular modeling data has elegantly allowed us to directly visualize the interaction of Hop1 ZnF with the Holliday junction. These studies suggest that recognition of the junction center is achieved by basic residues in the α-helix of Hop1 ZnF through a complex network of contacts with the sugar−phosphate backbone of the DNA. The role of Hop1 ZnF in Holliday junction resolution is emphasized by our comparison with the RecG wedge domain. The Hop1 ZnF motif shows striking structural similarity to RecG wedge domain, suggesting the possibility that Hop1 might have evolved from a RecG-like protein. Collectively, these results suggest that Hop1 ZnF can be regarded as both a strand separation module and a processivity factor.

What might be the biochemical role of Hop1 ZnF in homologue pairing? A scenario is now emerging in which *HOP1* plays an active role in enforcing meiotic recombination checkpoint control over the progression of recombination intermediates and interstitial pairing of meiotic chromosomes (*11*, *12*, *59*). The Holliday junction and other DNA substrates used in this study are bona fide intermediates of meiotic recombination, raising the possibility that ZnF motif could be the structural determinant involved in directing the native Hop1 protein to sites of branch migration and genetic exchange. The functional characterization of Hop1 ZnF will be useful in understanding its ability to distinguish different recombination intermediates as well as in elucidating the mechanism of its interaction with DNA substrates. Nonetheless, Hop1 ZnF offers a model for the design of ZnF motifs with further optimization of the amino acid residues and their interaction with the Holliday junction.

REFERENCES

1. Klug, A., and Schwabe, J. W. (1995) Zinc Fingers, *FASEB J. 9*, 597−604.
2. Pabo, C. O., Peisach, E., and Grant, R. A. (2001) Design and selection of novel Cys2His2 zinc finger proteins, *Annu. Rev. Biochem. 70*, 313−340.
3. Iuchi, S., and Kudell, N. (2004) *Zinc finger proteins: from atomic contact to cellular function*, Landes Biosciences, Georgetown, TX.
4. Dhanasekaran, M., Negi, S., and Sugiura, Y (2006) Designer zinc finger proteins: Tools for creating artificial DNA-binding functional proteins, *Acc. Chem. Res. 39*, 45−52.
5. Landers, E. S., Linton, L. M., Birren, B., Nusbaum, C., Zody, M. C., Baldwin, J., et al. (2001) Initial sequencing and analysis of the human genome, *Nature 409*, 860−921.
6. Clarke, N. D., and Berg, J. M. (1998) Zinc fingers in *Caenorhabditis elegans*: finding families and probing pathways, *Science 282*, 2018−2022.
7. Vallee, B. L., Coleman, J. E., and Auld, D. S. (1991) Zinc fingers, zinc clusters, and zinc twists in DNA-binding protein domains, *Proc. Natl. Acad. Sci. U.S.A. 88*, 999−1003.
8. MacPherson, S., Larochelle, M., and Turcotte, B. (2006) A fungal family of transcriptional regulators: the zinc cluster proteins, *Microbiol. Mol. Biol. Rev. 70*, 583−604.
9. Pedone, P. V., Ghirlando, R., Clore, G. M., Gronenborn, A. M., Felsenfeld, G., and Omichinski, J. G. (1996) The single Cys2-His2 zinc finger domain of the GAGA protein flanked by basic residues is sufficient for high affinity specific DNA binding, *Proc. Natl. Acad. Sci. U.S.A. 93*, 2822−2826.
10. Dathan, N., Zaccaro, L., Esposito, S., Isernia, C., Omichinski, J. G., Riccio, A., Pedone, C., Di Blasio, B., Fattorusso, R., and Pedone, P. V. (2002) The *Arabidopsis* SUPERMAN protein is able to specifically bind DNA through its single Cys2-His2 zinc finger motif, *Nucleic Acids Res. 30*, 4945−4951.
11. Hollingsworth, N. M., and Byers, B. (1989) *HOP1*: a yeast meiotic pairing gene, *Genetics 121*, 445−462.
12. Woltering, D., Baumgartner, B., Bagchi, S., Larkin, B., Loidl, J., de los Santos, T., and Hollingsworth, N. M. (2000) Meiotic segregation, synapsis, and recombination checkpoint functions require physical interaction between the chromosomal proteins Red1p and Hop1p, *Mol. Cell. Biol. 20*, 6646−6658.
13. Schwacha, A., and Kleckner, N. (1994) Identification of joint molecules that form frequently between homologs but rarely between sister chromatids during yeast meiosis, *Cell 76*, 51−63.
14. Mao-Draayer, Y., Galbraith, A. M., Pittman, D. L., Cool, M., and Malone, R. E. (1996) Analysis of meiotic recombination pathways in the yeast *Saccharomyces cerevisiae*, *Genetics 144*, 71−86.
15. Anuradha, S., and Muniyappa, K. (2005) Molecular aspects of meiotic chromosome synapsis and recombination, *Prog. Nucleic Acids Res. Mol. Biol. 79*, 49−132.
16. Hollingsworth, N. M., Goetsch, L., and Byers, B. (1990) The *HOP1* gene encodes a meiosis-specific component of yeast chromosomes, *Cell 61*, 73−84.
17. Couteau, F., Goodyear, W., and Zetka, M. (2004) Finding and keeping your partner during meiosis, *Cell Cycle 3*, 1014−1016.
18. Smith, A. V., and Roeder, G. S. (1997). The yeast Red1 protein localizes to the cores of meiotic chromosomes, *J. Cell Biol. 136*, 957−967.
19. Hollingsworth, N. M., and Ponte, L. (1997). Genetic interactions between *HOP1*, *RED1* and *MEK1* suggest that *MEK1* regulates assembly of axial element components during meiosis in the yeast *Saccharomyces cerevisiae*, *Genetics 147*, 33−42.
20. Kironmai, K. M., Muniyappa, K., Friedman, D. B., Hollingsworth, N. M., and Byers, B. (1998) DNA-binding activities of Hop1 protein, a synaptonemal complex component from *Saccharomyces cerevisiae*, *Mol. Cell. Biol. 18*, 1424−1435.
21. Freidman, D. B., Hollingsworth, N. M., and Byers, B. (1994) Insertional mutations in the yeast *HOP1* gene: evidence for multimeric assembly in meiosis, *Genetics 136*, 449−464.
22. Tripathi, P., Anuradha, S., Ghosal, G., and Muniyappa, K. (2006) Selective Binding of Meiosis-specific Yeast Hop1 Protein to the Holliday Junctions Distorts the DNA Structure and Its Implications for Junction Migration and Resolution, *J. Mol. Biol. 364*, 599−611.
23. Duckett, D. R., Murchie, A. I., Diekmann, S., von Kitzing, E., Kemper, B., and Lilley, D. M. (1988) The structure of the Holliday junction and its resolution, *Cell 55*, 79−89.
24. Duckett, D. R., and Lilley, D. M. (1990) The three-way DNA junction is a Y-shaped molecule in which there is no helix-helix stacking, *EMBO J. 9*, 1659−1664.
25. Janscak, P., Garcia, P. L., Hamburger, F., Makuta, Y., Shiraishi, K., Imai, Y., Ikeda, H., and Bickle, T. A. (2003) Characterization and mutational analysis of the RecQ core of the bloom syndrome protein, *J. Mol. Biol. 330*, 29−42.
26. Sambrook, J., Fritsch, E. F., and Maniatis, T. (1989) *Molecular Cloning: a laboratory manual*, 2nd Ed., Cold Spring Harbor Laboratory Press, Cold Spring Harbor, NY.
27. Nesterenko, M. V., Tilley, J., and Upton, S. J. (1994) A simple modification of Blum's silver stain method allows for 30 minute detection of proteins in polyacrylamide gels, *J. Biochem. Biophys. Methods 28*, 239−242.
28. Maxam, A. M., and Gilbert, W. (1980) Sequencing end-labeled DNA with base-specific chemical cleavages, *Methods Enzymol. 65*, 499−560.
29. McGuffin, L. J., and Jones, D. T. (2003) Improvement of the GenTHREADER method for genomic fold recognition, *Bioinformatics 19*, 874−881.
30. Kelley, L. A., MacCallum, R. M., and Sternberg, M. J. E. (2000) Enhanced Genome Annotation using Structural Profiles in the Program 3D-PSSM, *J. Mol. Biol. 299*, 499−520.

31. Mallick, P., Weiss, R., and Eisenberg, D. (2002) The directional atomic solvation energy: an atom-based potential for the assignment of protein sequences to known folds, *Proc. Natl. Acad. Sci. U.S.A. 99*, 16041−16046.
32. Brennan, R. G., and Matthews, B. W. (1989) The helix-turn-helix DNA binding motif, *J. Biol. Chem. 264*, 1903−1906.
33. Anuradha, S., and Muniyappa, K. (2004) *Saccharomyces cerevisiae* Hop1 zinc finger motif is the minimal region required for its function *in vitro*, *J. Biol. Chem. 279*, 28961−28969.
34. Giraud-Panis, M.-J. E., and Lilley, D. M. J. (1998) Structural recognition and distortion by the DNA junction-resolving enzyme RusA, *J. Mol. Biol. 278*, 117−133.
35. Kepple, K. V., Boldt, J. L., and Segall, A M. (2005) Holliday junction-binding peptides inhibit distinct junction-processing enzymes, *Proc. Natl. Acad. Sci. U.S.A. 102*, 6867−6872.
36. Ghosh, K., Lau, C. K., Guao, F., Segall, A. M., and Van Duyne, G. D. (2005) Peptide trapping of the Holliday junction intermediate in Cre-loxP site-specific recombination, *J. Biol. Chem. 280*, 8290−8299.
37. Fujimoto, D. F., Pinilla, C., and Segall, A. M. (2006) New peptide inhibitors of type IB topoisomerases: similarities and differences vis-a-vis inhibitors of tyrosine recombinases, *J. Mol. Biol. 363*, 891−907.
38. Carey, J. (1991) Gel retardation, *Methods Enzymol. 208*, 103−117.
39. Ho, P. S., and Eichman, B. F. (2001) The crystal structures of DNA Holliday junctions, *Curr. Opin. Struct. Biol. 11*, 302−308.
40. McKinney, S. A., DeClais, A.-C., Lilley, D. M. J., and Ha, T. (2003) Structural dynamics of individual Holliday junctions, *Nat. Struct. Biol. 10*, 93−97.
41. Churchill, M. E. A. (2003) Watching flipping junctions, *Nat. Struct. Biol. 10*, 73−75.
42. Iida, S., and Hayatsu, H. (1971) The permanganate oxidation of thymidine and thymidylic acid, *Biochim. Biophys. Acta 228*, 1−8.
43. DeClais, A.-C., and Lilley, D. M. J. (2000) Extensive central disruption of a four-way junction on binding CCE1 resolving enzyme, *J. Mol. Biol. 296*, 421−433.
44. West, S. C. (2003). Molecular views of recombination proteins and their control, *Nat. Rev. Mol. Cell Biol. 4*, 435−445.
45. Laity, J. H., Lee, B. M., and Wright, P. E. (2001) Zinc finger proteins: new insights into structural and functional diversity, *Curr. Opin. Struct. Biol. 11*, 39−46.
46. Wintjens, R., and Rooman, M. (1996) Structural classification of HTH DNA-binding domains and protein-DNA interaction modes, *J. Mol. Biol. 262*, 294−313.
47. Krishna, S. S, Majumdar, I., and Grishin, N.V. (2003) Structural classification of zinc fingers, *Nucleic Acids Res. 31*, 532−550.
48. Jeruzalmi, D., O'Donnell, M., and Kuriyan, J. (2001) Crystal structure of the processivity clamp loader gamma complex of *E. coli* DNA polymerase III, *Cell 106*, 429−441.
49. Singleton, M. R., Scaife, S., and Wigley, D. B. (2001) Structural analysis of DNA replication fork reversal by RecG, *Cell 107*, 79−89.
50. Briggs, G. S., Mahdi, A. A., Wen, Q., and Lloyd, R. G. (2005) DNA binding by the substrate specificity (wedge) domain of RecG helicase suggests a role in processivity, *J. Biol. Chem. 280*, 13921−13927.
51. Mahdi, A. A., McGlynn, P., Levett, S. D., and Lloyd, R. G. (1997) DNA binding and helicase domains of the *Escherichia coli* recombination protein RecG, *Nucleic Acids Res. 25*, 3875−3880.
52. Schaub, M., Krol, A., and Carbon, P. (1999) Flexible zinc finger requirement for binding of the transcriptional activator staf to U6 small nuclear RNA and tRNA(Sec) promoters, *J. Biol. Chem. 274*, 24241−24249.
53. Friesen, W. J., and Darby, M. K. (1998) Specific RNA binding proteins constructed from zinc fingers, *Nat. Struct. Biol. 5*, 543−546.
54. Wang, B. S., and Pabo, C. O. (1999) Dimerization of zinc fingers mediated by peptides evolved in vitro from random sequences, *Proc. Natl. Acad. Sci. U.S.A. 96*, 9568−9573.
55. Pedone, P. V., Omichinski, J. G., Nony, P., Trainor, C., Gronenborn, A. M., Clore, G. M., and Felsenfeld, G. (1997) The N-terminal fingers of chicken GATA-2 and GATA-3 are independent sequence-specific DNA binding domains, *EMBO J. 16*, 2874−2882.
56. Omichinski, J. G., Pedone, P. V., Felsenfeld, G., Gronenborn, A. M., and Clore, G. M. (1997) The solution structure of a specific GAGA factor-DNA complex reveals a modular binding mode, *Nat. Struct. Biol. 4*, 122−130.
57. Lu, D., Searles, M. A., and Klug, A. (2003) Crystal structure of a zinc-finger−RNA complex reveals two modes of molecular recognition, *Nature 426*, 96−100.
58. Omichinski, J. G., Clore, G. M., Schaad, O., Felsenfeld, G., Trainor, C., Appella, E., Stahl, S. J., and Gronenborn, A. M. (1993) NMR structure of a specific DNA complex of Zn-containing DNA binding domain of GATA-1, *Science 261*, 438−446.
59. Anuradha, S., Tripathi, P., Mahajan, K., and Muniyappa, K. (2005) Meiosis-specific yeast Hop1 protein promotes pairing of double-stranded DNA helices via G/C isochors, *Biochem. Biophys. Res. Commun. 336*, 934−941.
60. DeLano, W. L. (2002) The PyMOL User's Manual, DeLano Scientific, Palo Alto, CA.

BI701078V